Eur. Phys. J. C (2020) 80:562
https://doi.org/10.1140/epjc/s10052-020-8120-6

THE EUROPEAN PHYSICAL JOURNAL C

Regular Article - Theoretical Physics

Observational constraints on the non-flat ΛCDM model and a null test using the transition redshift

A. M. Velasquez-Toribio[a], **A. dos R Magnago**[b]

Departamento de Física, Nucleo Cosmo-ufes, Universidade Federal do Espirito Santo, Vitória, ES 29075-910, Brasil

Received: 8 January 2020 / Accepted: 7 June 2020 / Published online: 22 June 2020

Abstract A natural extension of the standard cosmological model are models that include curvature as a free parameter. In this work we study in detail the observational constraints on the non-flat ΛCDM model using the two main geometric tests: SNIa and Hubble parameter measurements. In general we show that the observational constraints on the parameters of the ΛCDM model strongly depend on the curvature parameter. In particular, we study the constraints on the transition redshift (z_t) of a universe dominated by matter for a universe dominated by the cosmological constant. Using this observable we construct a new null test defining $\zeta = z_{t,flat} - z_{t,nonflat}$. This test depends only on the data of the Hubble parameter, the Hubble constant and the matter density parameter. However, it does not depend on derivative of an observable as generally many tests in the literature. To reconstruct this test, we use the Gaussian process method. When we use the best-fit parameters values of $PLANCK/2018$, we find no evidence of a disagreement between the data and the standard model (flat ΛCDM), but if we use the value H_0 from $RIESS/2018$ we found a disagreement with respect at the standard model. However, it is important to note that the Hubble parameter data has large errors for a solid statistical analysis.

1 Introduction

The standard cosmology model is the ΛCDM model with flat spatial curvature. From the theoretical point of view, this model is the simplest explanation of the accelerating expansion of the universe [1,2] and is the model that best fits the different types of observational data: SNIa, BAO, CMB, Hubble parameter measurements, etc [3–7].

In particular, the recent results of the PLANCK collaboration have increased an intense debate on the curvature of the Universe, since the PLANCK results show statistical consistency with positive curvature models, i.e. closed universes. However, the observational constraints for non-flat models using Planck data are ambiguous, because there is no physically consistent inflationary model for the spectrum used by Planck. [1]

This evidence for closed models is observed when considering data of CMB lensing. Planck's collaboration [6] found more lensing effect than expected and to quantify this result, the A_{lens} parameter was introduced. In the reference [13] it is considered that if the curvature is included, then CMB lensing data indicates that the best fit corresponds to a closed universe at more than 99% C.L.

In this same line of research in the reference [14] the author claims a new cosmological tension, curvature tension. The author explicitly shows that the predictions for the curvature parameter using BAO, CMB lensing measurements and data of the $SH0ES$ Collaboration [15] are incompatible with each other. However, in the reference [16] the authors using a subsample of data of CMB lensing have confirmed a trend for a closed universe, but, when adding BAO data, the standard model remains the best fit. Another two recientes inconsistencies with respect at standard model are the tension of the Hubble constant using CMB data and low redshift data [17] and the data of cosmic shear of $KiDs$-450 measurements [18,19].

On the other hand, many other investigations using different types of data such as BAO data, $f\sigma_8$, SNIa and small-angles CMB have also shown this compatibility with closed models. For details to review the references: [20–30]. More recently the references [31,32] have investigated observa-

[a] e-mail: alan.toribio@ufes.br (corresponding author)

[b] e-mail: armagnago@gmail.com

[1] From the theoretical side, it is interesting to note that inflationary models for open and closed spaces have been proposed and investigated for quite some time, see references [8] and [9,10]. In particular Ratra has recently calculated the power spectrum for a closed universe in detail, see reference [11] and [12].

tional constraints using high-redshift QSO data and also verified statistical consistency of the data with closed models.

Additionally, in the literature different aspects have been investigated involving the curvature parameter such as: the equivalence between ΛCDM models with curvature and dynamic dark energy models [33–36]. The influence of the curvature on the observational constraints of the equation of state [37]. Also the model-independent approaches has been used to place observational constraints on the curvature: for example, the reference [38] use the luminosity distance and in the reference [39] the gravitational-wave standard sirens method is used.[2] The gravitational lenses have also been used to determine constraints on the curvature, see reference [43].[3] All these investigations show an intense activity to understand the effect of the curvature on the evolution of the Universe.

Independently if future observations demonstrate that the data are compatible with the flat ΛCDM model or alternatives models this current polemic places to the curvature parameter in an important position in the cosmological discussion. From the historical point of view the question of introducing the curvature parameter in a cosmological model is old, can be traced back to Einstein and De Sitter [44]. In this article they considered a Universe with finite matter density, in a homogeneous and isotropic model. The authors conclude that the observational data available at the time do not imply introducing the curvature, but mention that future data should allow limiting curvature values.

On the other hand, a phenomenological parameter that allows to characterize the accelerated expansion of any cosmological model is the deceleration parameter, which in turn allows us to study the redshift of the transition from a decelerated universe to an accelerated universe. This parameter has been quite studied in the ΛCDM model using the deceleration parameter [45].

The first real measurement of the transition redshift was described in the references [46,47] by Farooq et al. using different statistical techniques.[4] However, the determination of the transition redshift including curvature as a free parameter has been little investigated, with the exception of references [48,49] where a detailed analysis of the transition redshift for different non-flat models.

Motivated by all these recent results, in the present work, we study observational constraints on the transition redshift in the non-flat ΛCDM model using two geometric tests: SNIa data and Hubble parameter measurements.

Considering that the transition redshift in the non-flat ΛCDM model has an analytical expression, we can rewrite the Hubble parameter directly as a function of the transition redshift and the curvature parameter. In this way we avoid an extra propagation of errors. Additionally, it is important to note that we get quite general results, because to construct the confidence contours, we do not fix the values of the parameters, but use a marginalization process in a given range of values for the parameters.

Also, using the concept of transition redshift, we propose a new null test, which for the non-flat ΛCDM model explicitly depends on the Hubble parameter, the Hubble constant and the matter density parameter today. We use observational data from the Hubble parameter to reconstruct the expression of this test. In this we used as a statistical method the non-parametric method of Gaussian processes. We demonstrate that this test is strongly sensitive to the values of the parameters cosmological: (Ω_{m0}, H_0). It is important to note that this test is only valid to compare the flat and non-flat ΛCDM models. But in principle following the same idea similar tests can be built for other cosmological models.

Our paper is organized as follows. In Sect. 2 we summarize the cosmological dynamics of the non-flat ΛCDM model. In Sect. 3 we present a new null test using the transition redshift in Sect. 5 we present our data and in the Sect. 6 we present our result and conclusions.

2 The ΛCDM model in the background

Considering the cosmological principle, the FLRW metric can be written as [50–53],

$$ds^2 = -dt^2 + a(t)^2\left[\frac{dr^2}{1-kr^2} + r^2 d\theta^2 + r^2\sin^2\theta d\phi^2\right], \tag{1}$$

where $a(t)$ is the scale factor and k is the spatial curvature which can be $k = +1$ for a closed universe, $k = 0$ for a flat Universe and $k = -1$ for an open universe. In addition, if we consider Einstein's equations and a tensor energy-momentum of perfect fluid, then we can derive the fundamental equation of cosmology [54],

$$H^2 = \left(\frac{\dot{a}}{a}\right)^2 = \frac{8\pi G\rho}{3} + \frac{\Lambda}{3} - \frac{k}{a^2}. \tag{2}$$

This equation can be rewritten using the redshift as:

$$H = H_0\sqrt{\Omega_{m0}(1+z)^3 + \Omega_{k0}(1+z)^2 + \Omega_{\Lambda 0}}, \tag{3}$$

[2] It is interesting to mention that the application of gravitational waves in cosmology as a method to determine the Hubble constant begins with Schutz's proposal, [40].

[3] The statistics of gravitational lenses as a cosmological test and its relationship with the curvature parameter were developed by Park and Gott [41] and by Helbig [42].

[4] In the second reference they use the weighted mean and median statistics techniques.

where we use the definitions:

$$\Omega_{m0} = \frac{8\pi G\rho_{m0}}{3H_0^2},\ \Omega_{\Lambda 0} = \frac{\Lambda}{3H_0^2} \text{ and } \Omega_{k0} = \frac{-k}{a^2H^2}. \tag{4}$$

Additionally, we have the restriction:

$$\Omega_{m0} + \Omega_{\Lambda 0} + \Omega_{k0} = 1. \tag{5}$$

To calculate the transition redshift, z_t, of a decelerated to accelerated universe we use the definition of the deceleration parameter,

$$q(z) = -\frac{\ddot{a}}{aH^2} = \frac{d}{dt}\left(\frac{1}{H}\right) - 1. \tag{6}$$

Thus, using the definition of $H(z)$ and the condition for the transition redshift $q(z_t) = 0$. We can determine that [55],

$$z_t(\Omega_{m0}, \Omega_{k0}) = \left(\frac{2\Omega_{\Lambda 0}}{\Omega_{m0}}\right)^{1/3} - 1 \tag{7}$$

$$= \left(\frac{2\,(1 - \Omega_{m0} - \Omega_{k0})}{\Omega_{m0}}\right)^{1/3} - 1, \tag{8}$$

where we can observe that the transition redshift for a non-flat universe ΛCDM is a analytical function of the parameters of relative densities [55]. Using Eqs. (5) and (7) we can explicitly rewrite the hubble parameter using the variables, (Ω_{k0} e z_t) as,

$$H = H_0\sqrt{\frac{(1-\Omega_{k0})(1+z)^3}{\frac{1}{2}(1+z_t)+1} + \Omega_{k0}(1+z)^2 + \frac{(1-\Omega_{k0})(1+z_t)^3}{2(\frac{1}{2}(1+z_t)+1)}}. \tag{9}$$

We can also use the variables (Ω_{m0}, z_t) to write:

$$H = H_0\sqrt{\Omega_{m0}(1+z)^3 + (1-\Omega_{m0}(1+\frac{(1+z_t)^3}{2}))(1+z)^2 + \frac{\Omega_{m0}}{2}(1+z_t)^3}. \tag{10}$$

This expression of the Hubble parameter is important because the statistics of the χ^2 constructed will explicitly depend on these parameters avoiding a extra propagation of errors. The importance of the curvature parameter in determining the transition redshift can best be observed by means of Fig. 1. where we show the function $z_t(\Omega_{m0}, \Omega_{k0})$. This function is a well-behaved three-dimensional surface, except for extreme values of curvature and very low values of matter. But these regions are excluded by observational data. In the figure the intersection of the planes corresponds to the case where the curvature is zero. A quick inspection allows us to observe that if we consider curvature, then there are different ways to accommodate the measures on the surface of z_t. In particular if we consider that the observations various determine z_t preferably in the range (0.5–1.00), then the inclusion of the curvature allows that the value of z_t can easily be accommodated outside of the line for a flat universe. In this work we study the constraints associated with this degeneracy using SNIa and Hubble parameter measurements.

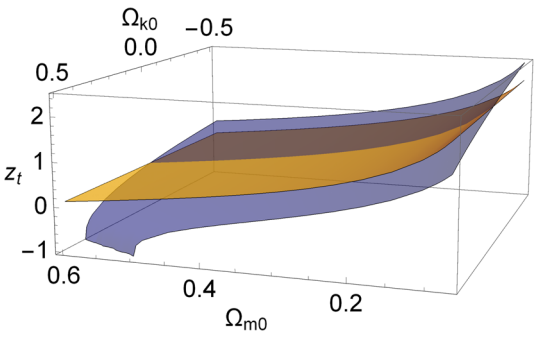

Fig. 1 The blue surface represents the transition redshift as a function of matter and curvature parameters in the non-flat model ΛCDM and the intersection of this curve with the yellow curve represents the transition redshift of the flat ΛCDM model

3 Null test for ΛCDM

We can define a new null test to distinguish between flat and non-flat ΛCDM models using the redshift transition. To do this we put in evidence the z_t of the expression for the Hubble parameter given by the Eq. (10) obtaining,

$$z_{t,non-flat} = \left(\frac{\left(\frac{H}{H_0}\right)^2 - \Omega_{m0}(1+z)^3 - (1-\Omega_{m0})\,(1+z)^2}{\Omega_{m0}\left(1-(1+z)^2\right)}\right)^{1/3} - 1, \tag{11}$$

In an analogous way we can determine for flat transition redshift, so the null test can be formulated as:

$$\zeta = z_{t,flat} - z_{t,nonflat}, \tag{12}$$

where we can see that if $\zeta = 0$, then the flat model is preferred, otherwise the model with curvature is preferred. It is important to note that this test definition is only valid for flat and non-flat ΛCDM model. However, this same idea can be extrapolated to other models with their appropriate definitions. In an explicit way we can write this null test as,

$$\zeta = \left(\frac{(\frac{H}{H_0})^2 - \Omega_{m0}(1+z)^3}{\Omega_{m0}}\right)^{1/3} - \left(\frac{(\frac{H}{H_0})^2 - \Omega_{m0}(1+z)^3 - (1-\Omega_{m0})(1+z)^2}{\Omega_{m0}(1-(1+z)^2)}\right)^{1/3}. \tag{13}$$

Interestingly, our test includes the reconstructed data of the Hubble parameter and does not include derivatives of data such as other tests, for example [56]. Data derivatives in general are difficult to obtain and spread the error remarkably.

However, our test explicitly includes the Hubble constant, H_0, and the matter density parameter today Ω_{m0}.

To reconstruct the observable, $H(z)$, we use only data from the Hubble parameter and as a statistical method we use the non-parametric method of Gaussian processes. This method is suitable for this case, since it does not assume a specific model to reconstruct the function $H(z)$. Once the $H(z)$ function is obtained, the null test can be reconstructed. As a first approximation to determine the errors of the ζ function we can use the theory of error propagation,

$$\sigma_\zeta = \sqrt{\frac{\partial\zeta}{\partial H}\delta H + \frac{\partial\zeta}{\partial H_0}\delta H_0 + \frac{\partial\zeta}{\partial\Omega_{m0}}\delta\Omega_{m0}}. \tag{14}$$

To perform the reconstruction of Gaussian processes we use the popular public package $GaPP$, which has been applied to a large number of cosmological studies. For package details you can see the references [57]. For a recent use of this package to see the reference [58].

4 Observational constraints

For determine observational constraints on the non-flat ΛCDM model it is essential to define the comoving distance as,

$$r(z) = \frac{c}{H_0}\int_0^z \frac{dz'}{E(z')}. \tag{15}$$

To determine the luminosity distance including curvature is necessary to distinguish three cases, for this we define the transversal comoving distance, r_t,[5]

$$r_t = \begin{cases} \frac{c}{H_0}\frac{1}{\sqrt{\Omega_{k0}}}\sinh\left[\sqrt{\Omega_{k0}}\frac{H_0}{c}r(z)\right] & \text{for } \Omega_{k0} > 0 \\ r(z) & \text{for } \Omega_{k0} = 0 \\ \frac{c}{H_0}\frac{1}{\sqrt{|\Omega_{k0}|}}\sin\left[\sqrt{|\Omega_{k0}|}\frac{H_0}{c}r(z)\right] & \text{for } \Omega_{k0} < 0 \end{cases} \tag{16}$$

using the above definitions we can determine the luminosity distance as,

$$d_L = (1+z)r_t \tag{17}$$

4.1 Supernovae Ia

In this study we use the data from Supernovas Ia called "Pantheon" sample [59] which is the largest combined sample of SNIa and consists of 1048 data with redshifts in the range $0.01 < z < 2.3$. It is a collection of SNe Ia discovered by the Pan-STARRS1 (PS1) Medium Deep Survey and SNe Ia from Low-z, SDSS, SNLS and HST surveys. This supernova Ia compilation uses The SALT 2 program to transform light curves into distances using a modified version of the Tripp formula [60],

$$\mu = m_B - M + \alpha x_1 - \beta c + \Delta_M + \Delta_B, \tag{18}$$

where μ is the distance modulus, Δ_M is a distance correction based on the host-galaxy mass of the SNIa and Δ_B is the distance correction based on predicted bias from simulations. Also α is the coefficient of the relation between luminosity and stretch, β is the coefficient of the relation between luminosity and color and M is the absolute B-band magnitude of a fiducial SNIa with $x_1 = 0$ and $c = 0$. Also c is the color and x_1 is the light-curve shape parameter and m_B is the log of the overall flux normalization. An uncertainty matrix $\mathbf{C}$ is defined such that,

$$\chi^2_{SNIa} = \Delta\boldsymbol{\mu}^T.\mathbf{C}^{-1}.\Delta\boldsymbol{\mu}, \tag{19}$$

where $\Delta\boldsymbol{\mu} = \boldsymbol{\mu}_{obs} - \boldsymbol{\mu}_{model}$ and $\boldsymbol{\mu}_{model}$ is a vector of distance modulus from a given cosmological model and $\boldsymbol{\mu}_{obs}$ is a vector of observational distance modulus. The $\boldsymbol{\mu} = \mathbf{m} - M$, where M is the absolute magnitude and $\mathbf{m}$ is the apparent magnitude, which is given by

$$\begin{aligned} \mathbf{m}_{model} &= M + 5Log_{10}(D_L) + 5Log_{10}(\frac{c/H_0}{1Mpc}) + 25 \\ &= \bar{M} + 25 + 5Log(D_L). \end{aligned} \tag{20}$$

where $D_L = \frac{H_0}{c}d_L$ and $\bar{M} = M + 5Log\left(\frac{c/H_0}{1Mpc}\right)$ is an nuisance parameter, which depends on the Hubble constant H_0 and the absolute magnitude M. To minimize with respect to the nuisance parameter we follow a process similar at the references [61,62]. Therefore the $\chi^2_{\bar{M}marg}$ is,

$$\chi^2_{\bar{M}marg} = a + \log\frac{e}{2\pi} - \frac{b^2}{e}, \tag{21}$$

where,

$$a = \Delta\mathbf{m}^T.C^{-1}.\Delta\mathbf{m}, \tag{22}$$

$$b = \Delta\mathbf{m}^T.C^{-1}.\mathbb{I}, \tag{23}$$

$$e = \mathbb{I}^T.C^{-1}.\mathbb{I} \tag{24}$$

where $\Delta\mathbf{m} = \mathbf{m}_{obs} - \mathbf{m}_{model}$ and $\mathbb{I}$ is the identity matrix.

4.2 Hubble parameter measurements

There are two efficient and widely used forms to obtain Hubble parameters measurements:

[5] Here we follow the notation of the article by D. Hogg see reference arXiv:astro-ph/9905116v4.

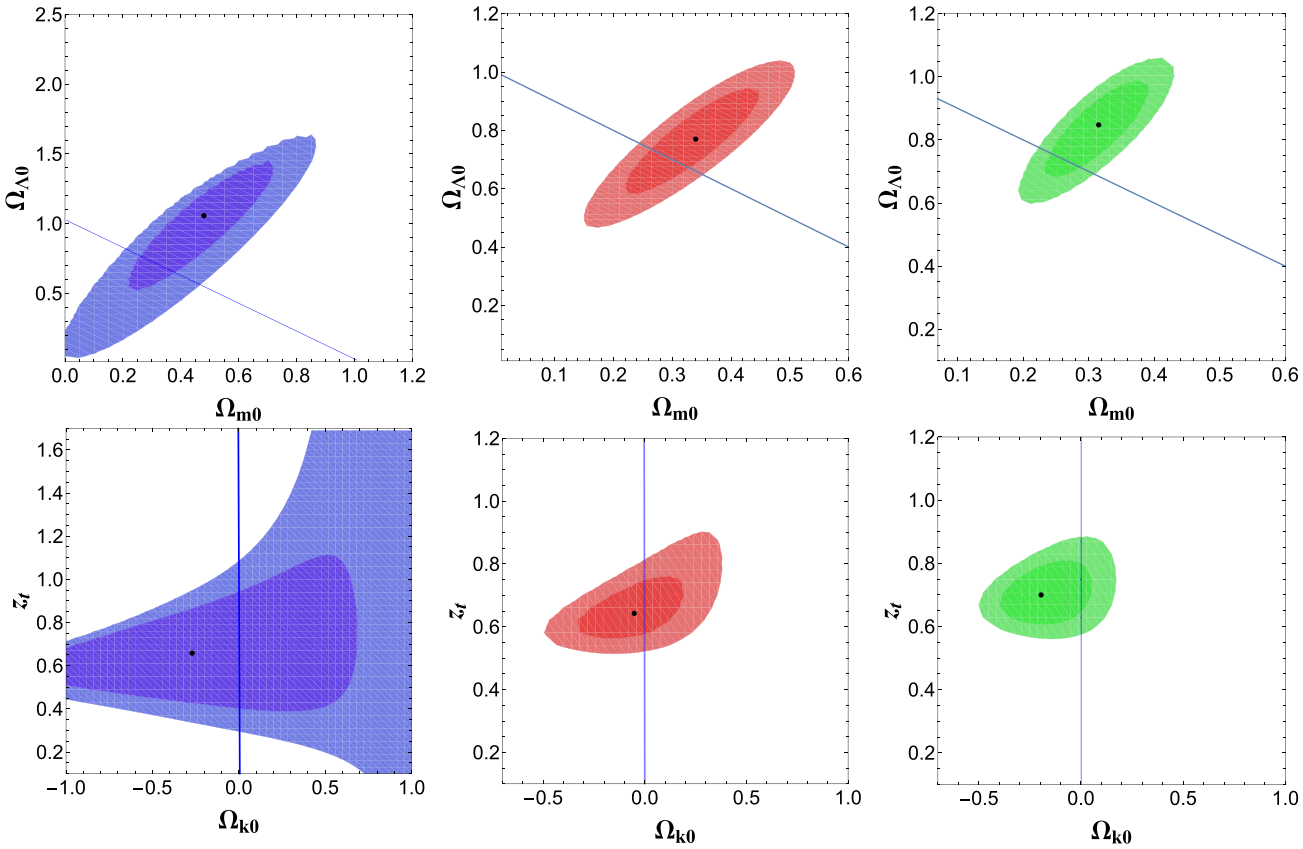

Fig. 2 Observational constraint using Hubble parameters measurements (left) and SNIa (middle). A joint analysis is shown on the right side. In all case we marginalized $50 < H_0 < 80$). The blue line represents the universe with flat curvature

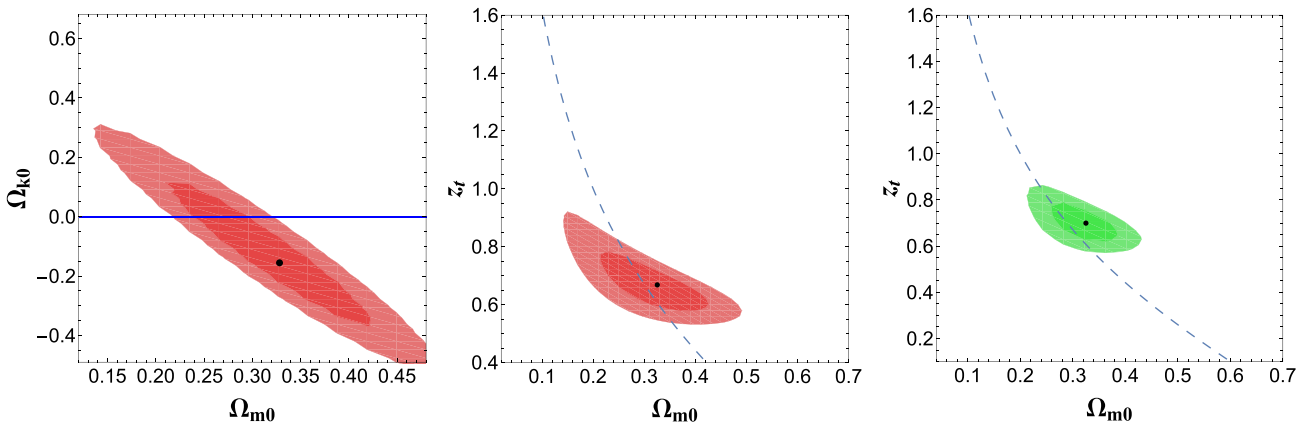

Fig. 3 In the figure on the left we show a strong degenerescence between the curvature parameter and the matter density parameter. In the central figure we show observational constraints updated for the parameter space studied in the reference [65] and on the right we show the joint data observational constraints. The green dashed line represents the universe with flat curvature

- Cosmic chronometers (CC): this method is based on the expression of the differential age of the universe as a function of redshift,

$$H(z) = -\frac{1}{1+z}\frac{dz}{dt}. \tag{25}$$

This method was proposed by directly measuring the amount dz/dt and, consequently, the Hubble parameter. The most used data to measure this amount have been passively evolving galaxies with high-resolution spectroscopic data along with synthetic catalogs to limit the

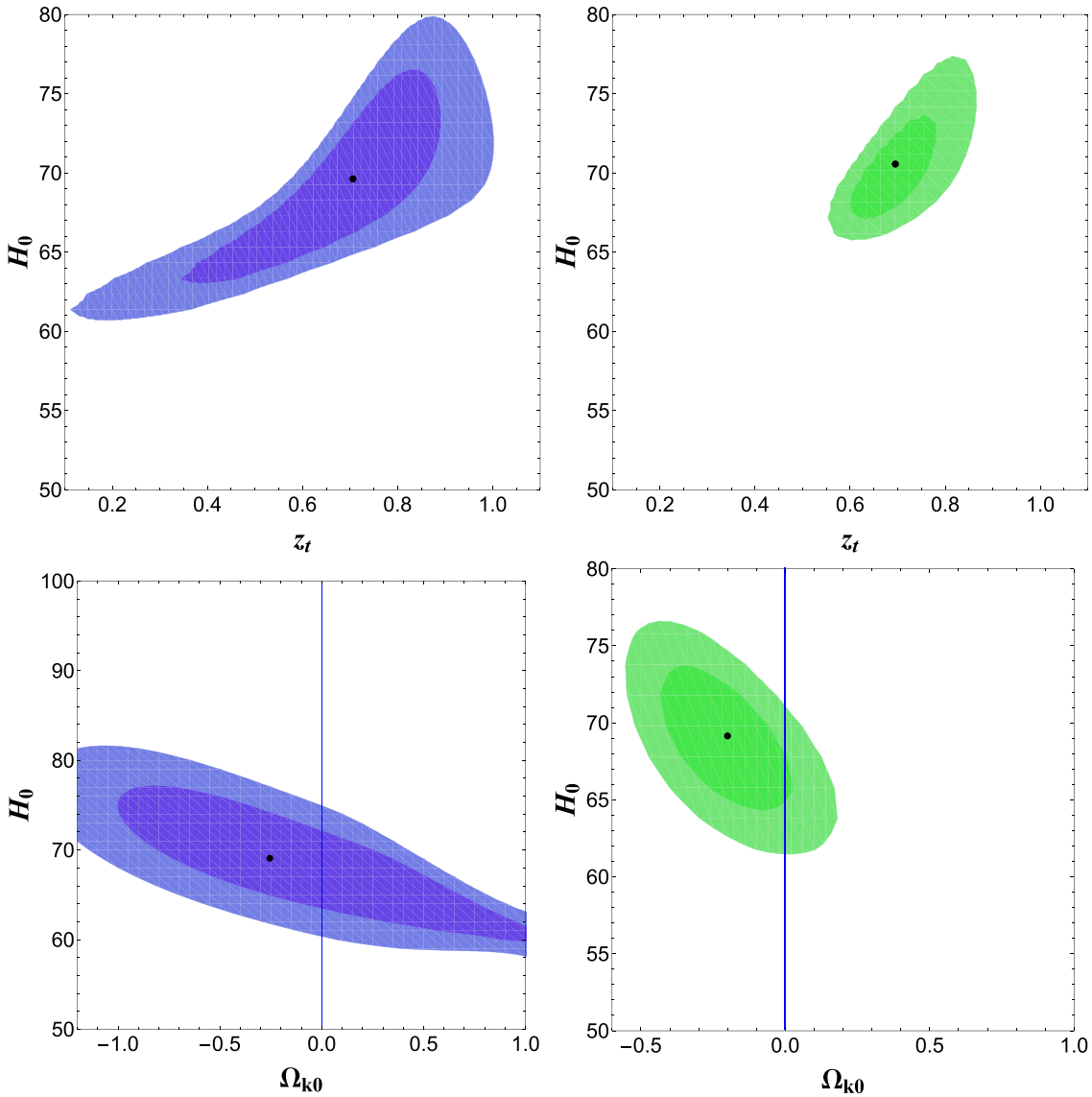

Fig. 4 In the figure on the left we show constraints on the Hubble constant using data from the Hubble parameter and on the left side we add data from Supernovas Ia. In all cases we marginalize the matter density parameter in the interval $0.07 < \Omega_{m0} < 0.6$

age of the oldest stars in the galaxy. A complete description of this methodology can be reviewed for the SDSS in the reference [63].

- The radial BAO size method: this method is based on measurements of the scale of BAO. This method is more accurate with respect to CC. This accuracy is understandable because BAO mainly depends on a spatial measurement compared to the first method where a time measure is required which increases systematic errors. However, this method of BAO requires assuming a prior in the radius of the sound horizon,$r(z)$, so that

$$H(z) = -\frac{r_{bao}(z)}{r_{cmb}(z)} H_{fiducial}(z). \tag{26}$$

This method depends on the fiducial model, usually the model associated with CMB is the ΛCDM model.

In the literature there are different compilations of samples of the Hubble parameters data, we use the sample presented by [64] what includes data of CC and BAO. From this sample the data at $z = 2.34$ and at $z = 0.4497$ are excluded. The first point is a measurement using the BAO technique and we have verified that it has a strong influence on the parameter estimation. As this measurement is very restrictive we have excluded this data. We believe that more data are required at high redshift using BAO and other techniques, such as the Sandage–Loeb effect, to have confidence in including high redshift data. On the other hand, the measurement in

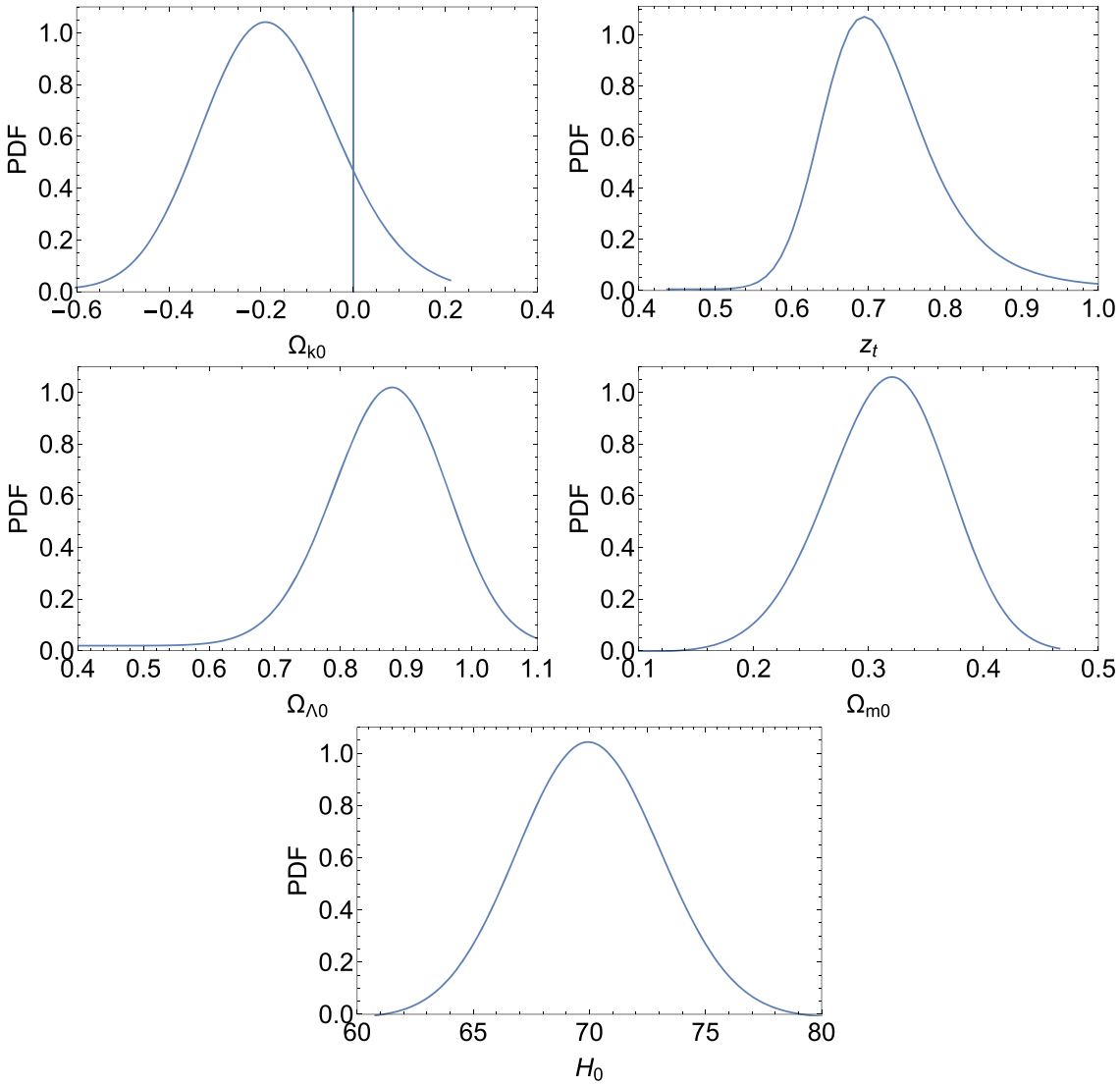

Fig. 5 In the figure we show the PDFs for all the observables involved in the ΛCDM background model

the redshift $z = 0.4497$, overlaps with another data and has a negligible effect on the results. Therefore, our sample has 34 points. With these considerations we have verified that our data approximate to more recent samples such as [26]. Our data cover a range $0.2 < z < 2.00$ in redshift. We can construct the statistics χ^2_H as,

$$\chi^2_H(\Omega_{m0}, \Omega_\Lambda, H_0) = \sum_{i=1}^{34} \frac{(H_{obs,i} - H_{model}(z_i, \Omega_{m0}, \Omega_\Lambda, H_0))^2}{\sigma^2_{obs,i}}, \quad (27)$$

where $H_{obs,i}$ are the observational data and H_{model} are the theoretical values determined by Eq. (2) and the $\sigma_{obs,i}$ are the errors of the observational data.

4.3 Combining data

We combine the data by adding the χ^2 of each dataset, so we get

$$\chi^2_{total}(\Omega_{m0}, \Omega_{\Lambda 0}, H_0) = \chi^2_{SNIa,marg} + \chi^2_H. \quad (28)$$

We can construct the probability contours through the marginalization process, thus, for example, for the case of $(\Omega_{m0}, \Omega_{\Lambda 0})$ we integrate on the likelihood with respect H_0,

$$L(\Omega_{m0}, \Omega_{\Lambda 0}) = -2Log_{10}\left[\int_{50}^{80} e^{-\frac{\chi^2_{total}(\Omega_{m0}, \Omega_{\Lambda 0}, H_0)}{2}} dH_0\right]. \quad (29)$$

For other sets of parameters we proceed analogously.

Table 1 Best-fitting parameters 1σ confidence intervals

Parameters	Best-fitting	Marginalization range
Ω_{m0}	0.325 ± 0.0750	$0.07 < \Omega_{m0} < 0.600$
H_0	70.06 ± 1.99	$50 < H_0 < 80$
z_t	0.69 ± 0.25	$0.400 < z_t < 1.00$
Ω_{k0}	-0.195 ± 0.210	$-0.50 < \Omega_{k0} < 0.50$

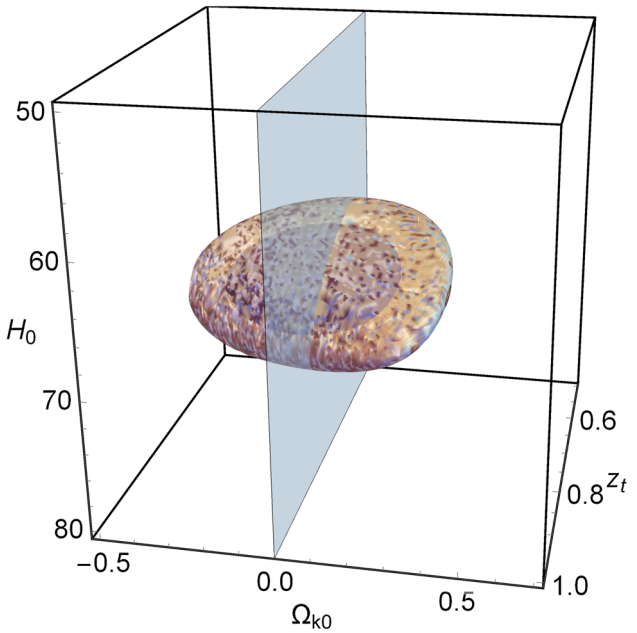

Fig. 6 The 1σ - 2σ confidence contour of the parameters space (z_t, Ω_{k0}, H_0) using the joint analysis

5 Results and discuss

We investigate the observational constraints on the different combinations of cosmological parameters. In Fig. 2, we show the observational constraints using SNIa and the Hubble parameter data. In all cases we use a marginalization over the Hubble parameter in the range $50 < H_0 < 80$. The figure on the right side show the constraints due to the sum of the data. It is worth mentioning the lower right figure, which shows the dependence between the curvature parameter and the transition redshift. But it is also evident that the flat model is within 1σ. The Fig. 3, on the left side, we show the strong degenerescence between the matter density parameter and the parameter of curvature for SNIa data, in the middle figure we show the confidence contours for the matter versus the transition redshift. This result updates the calculation shown in the reference [65]. The discontinuous curve represents the flat universe.

In Fig. 4 we show the dependence of the parameters with respect to the Hubble constant, H_0. For all cases we use a marginalization interval on the matter density parameter of

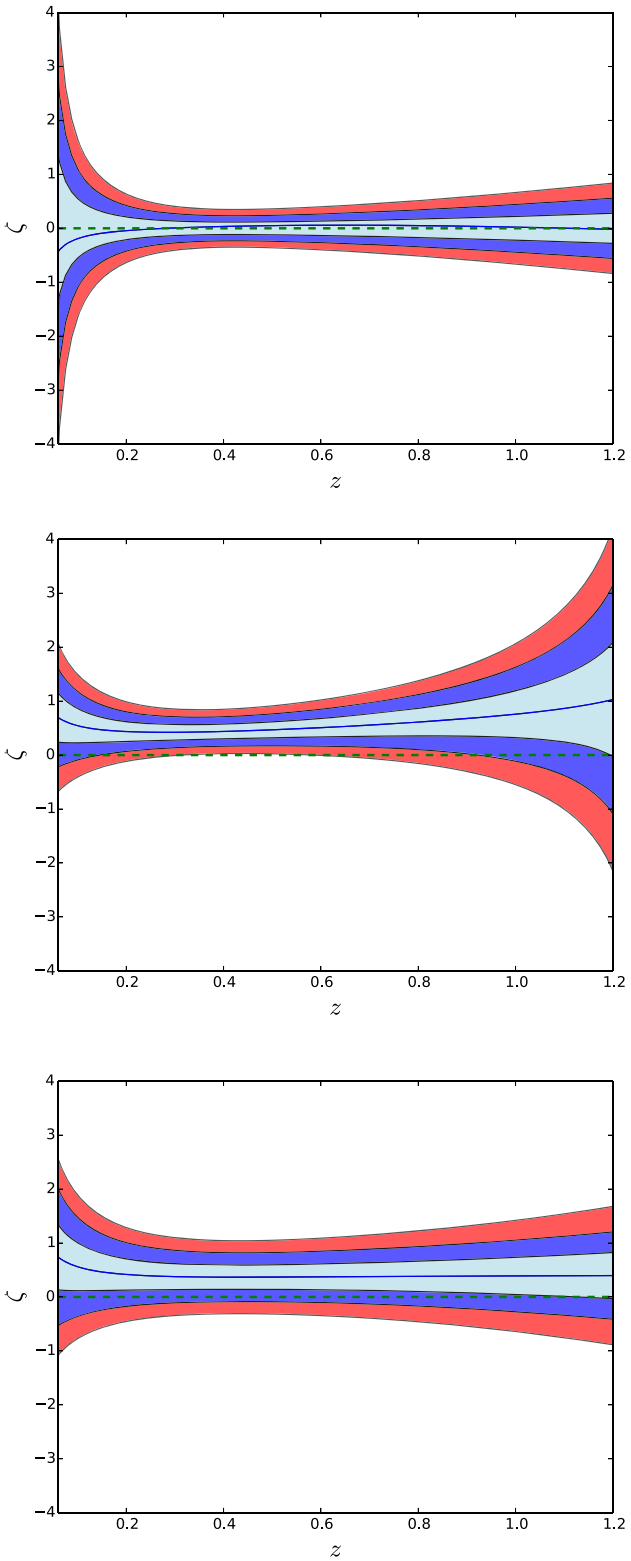

Fig. 7 The results for the reconstruction of the null test for the non-flat ΛCDM using Hubble parameters measurements with 1σ, 2σ and 3σ of C.L. In the figure above we can see the reconstruction of the null test using GP and the best-fit of PLANCK/2018. In the middle figure we show the reconstruction using the $H_0 = 74.03 \pm 1.42$ of RIESS et al./2018. In the figure below we maintain the value of the Hubble constant of RIESS et al. and use $\Omega_{m0} = 0.28 \pm 0.01$. The dashed line represents the flat ΛCDM model and the solid blue line represents the average value of the ζ test

$0.07 < \Omega_{m0} < 0.6$. On the right side we show the constraints of the sum $SNIa + H$. We can see that the variation range of, z_t, corresponds to $0.4 < z_t < 1.00$ and of the curvature parameter for $-0.2 < \Omega_{k0} < 0.2$. In Fig. 5, we show the PDFs for all the parameters studied. The best-fitting values are shown in Table 1 with 1σ. In Fig. 6, we show the three-dimensional constraints for the parameter space (Ω_{k0}, z_t, H_0). In this figure we shown that the geometric tests can restrict the parameters values on a closed surface for the non-flat ΛCDM model, but the flat model ΛCDM cannot be ruled out.

In Fig. 7 we shown the result of the null test using the Gaussian process method. In the figure on the left side we use the best-fitting values of the $PLANCK/2018$ [6],[6] $H_0 = 67.4 \pm 0.5$ and $\Omega_{m0} = 0.315 \pm 0.007$. We can see that the flat ΛCDM model adjusts the null test very well. However, if we use the local value of the Hubble constant of $RIESS$ et al./ 2018[17][7] $H_0 = 74.03 \pm 1.42$ and keep the same value of Ω_{m0} the null test at 2σ does not correspond to the flat ΛCDM model. On the other hand, if we use a smaller value of the parameter of matter, maintaining the value of H_0 of $RIESS$ et al., we can reconcile the flat ΛCDM model in 1σ. Combining this result with the results of table one, we can see that the results of the null test show that a high value of H_0 statistically favors a universe with closed curvature.

6 Conclusion

In the present work we have investigated the observational constraints on the non-flat ΛCDM model using as observational data the SNIa and Hubble data. We have emphasized the study on the transition redshift, which can be used to construct a null test. This test is sensitive to the values of $H(z)$, H_0 and Ω_{m0}, but does not include derivatives of cosmological observables, which prevents excessive propagation of errors.

In general, we have shown a strong dependence between the constraints of the curvature parameter and all other parameters. Our results, without considering our null test, are quite general, because we do not use fixed values of the parameters, but we have used a marginalization process integrating in a large interval to allow considerable changes of the parameters. In all case the flat ΛCDM model cannot be excluded. A subsequent study may include other observables such as BAO, QSO and structure growth data to constraints the transition redshift with curvature, i.e., the (z_t, Ω_{k0}) plane.

On the other hand, the null test is quite sensitive to the values of the parameters, for the best-fitting of Planck/2018 the flat ΛCDM model is preferred, but if use the Hubble constant value local of $Riess$ et al. 2018 our null test excludes the flat model with 2σ. If we consider values less for the matter content, for example, $\Omega_{m0} = 0.28$, we can alleviate the rejection of the flat model at 1σ. To reconstruct the null test we only use data from the Hubble parameter measurements and the non-parametric method of Gaussian processes. We do not include $SNIa$, since it would imply reconstruct derivatives and would spread the error excessively. Our null test may be interesting to study other cosmological models, such as a quintessence model or interaction between dark energy and dark matter models.

Acknowledgements A.M.V.T would like to thank the reading of the manuscript and suggestions made by J.C. Fabris. We also appreciate the computational facilities of the UFES to develop the work.

Data Availability Statement This manuscript has no associated data or the data will not be deposited. [Authors' comment: The SNIa datasets used during the current study are the data of the Scolnic et al. Supernova catalog available in the: https://archive.stsci.edu/prepds/ps1cosmo/ and the Hubble parameter data are available in the paper https://doi.org/10.3847/0004-637X/825/1/17, table I.]

Funded by SCOAP[3].

[6] Evidence for low values of H_0 has been published by different groups for some time, for example, to see the references [66] and [67], they have used the statistical technique of the median statistics and the Huchra's compilation of 553 measurements of the Hubble constant, the authors determined a $H_0 = 68 \pm 5 km/s/Mpc$. Other groups more recently have also determined results compatible with Planck's results, see references [68–75].

[7] Other research groups have also made local measurements of the Hubble parameter and have determined values compatible with the results of RIESS et al. For example, see [76–83]. Which measurement of H_0 is correct? This constitutes H_0 tension and is one of the topics under discussion in cosmology today. See, for example, the reference [84] and references therein.

References

1. S. Perlmutter et al., ApJ **517**, 565 (1999)
2. A. Riess et al., ApJ **116**, 1009 (1998)
3. Sean M. Carroll, Living Rev. Relat. **4**, 1 (2001). arXiv:astro-ph/0004075
4. P.J.E. Peebles, B. Ratra, Rev. Mod. Phys. **75**(2), 559–606 (2003). arXiv:astro-ph/0207347
5. M. Tanabashi et al., Particle Data Group. Phys. Rev. D **98**, 030001 (2018)
6. Planck Collaboration and N. Aghanim, et al., Planck results. VI. Cosmological parameters, (2018). arXiv:1807.06209

7. DES Collaboration, Phys. Rev. Lett. **122** 17, (2018). arXiv:1811.02375
8. J.R. Gott, Nature **295**, 304 (1982)
9. S. Hawking, Nucl. Phys. B **239**, 257 (1984)
10. B. Ratra, Phys. Rev. D **31**, 1931 (1985)
11. B. Ratra, Phys. Rev. D **52**, 1837 (1995)
12. B. Ratra, Phys. Rev. D **96**, 103534 (2017). arXiv:1707.03439
13. Di Valentino, E., Melchiorri, A. & Silk, J., Nat. Astron., (2019). arXiv:1911.02087
14. Handley, W. arxiv:1908.09139
15. SH0ES Collaboration, ApJ **855**, 136, (2018)
16. Efstathiou, G., & Gratton, S. arXiv:1910.00483
17. Riess, A. G., Casertano, S., Yuan, W., Macri, L. M. & Scolnic, D., ApJ **876** (1) 85, (2019). arXiv:1903.07603
18. H. Hildebrandt et al., MNRAS **465**, 1454 (2017). arXiv:1606.05338
19. Joudaki, S. et al., MNRAS **471** (2), 1259 (2017). arXiv:1610.04606
20. J. Ooba, B. Ratra, N. Sugiyama, ApJ **864**, 80 (2018). arXiv:1707.03452
21. J. Ooba, B. Ratra, N. Sugiyama, ApJ **866**, 68 (2018). arXiv:1710.03271
22. J. Ooba, B. Ratra, N. Sugiyama, ApJ **869**, 34 (2018). arXiv:1712.08617
23. C.-G. Park, B. Ratra, ApJ **868**, 83 (2018). arXiv:1807.07421
24. C.-G. Park, B. Ratra, ApSS **364**, 82 (2018). arXiv:1803.05522
25. C.-G. Park, B. Ratra, ApSS **364**, 134 (2019). arXiv:1809.03598
26. C.-G. Park, B. Ratra, ApJ **882**, 158 (2019). arXiv:1801.00213
27. C.-G. Park, B. Ratra, Phys. Rev. D **101**(8), 083508 (2020). arXiv:1908.08477
28. J. Ryan, S. Doshi, B. Ratra, MNRAS **480**, 759 (2018). arxiv:1805.06408
29. J. Ryan, Y. Chen, B. Ratra, MNRAS **488**(3), 3844 (2019)
30. W. Handley, Phys. Rev. D **100**, 123517 (2019)
31. N. Khadka, B. Ratra, MNRAS **492**(3), 4456 (2020). arXiv:1909.01400
32. Khadka N., Ratra B. arXiv:2004.09979
33. K. Ichikawa, M. Kawasaki, T. Sekiguchi, T. Takahashi, JCAP **0612**, 005 (2006). arXiv:astro-ph/0605481
34. K. Ichikawa, T. Takahashi, Phys. Rev. D **73**, 083526 (2006). arXiv:astro-ph/0511821
35. Ichikawa, K., & Takahashi, T. JCAP **0702**, 001 (2007). arXiv:astro-ph/0612739
36. Ichikawa, K., & Takahashi, T. JCAP **0804**, 027 (2008). arXiv:0710.3995
37. C. Clarkson, M. Corts, B. Bassett, JCAP **8**, 011 (2007)
38. C. Clarkson, B. Bassett, T.H.C. Lu, Phys. Rev. Lett. **101**, 011301 (2008)
39. J.J. Wei, ApJ **868**, 29 (2018)
40. B.F. Schutz, Nature **323**, 310 (1986)
41. M.G. Park, J.R. Gott, ApJ **489**, 476 (1997). arXiv:09702173
42. D.H. Han, M.G. Park, J. Korean Astron. Soc. **65**, 827 (2014)
43. A. Rana, D. Jain, S. Mahajan, A. Mukherjee, JCAP **3**, 028 (2017)
44. A. Einstein, W. de Sitter, Proc. Natl. Acad. Sci. USA **18**(3), 213–214 (1932)
45. E.E.O. Ishida, R.R.R. Reis, A.M. Toribio, I. Waga, Astropart. Phys. **28**, 547 (2008). arXiv:astro-ph/0706.0546
46. O. Farooq, B. Ratra, ApJ **766**, L7 (2013). arXiv:1301.5243
47. O. Farooq, S. Crandall, B. Ratra, Phys. Lett. B **726**, 72 (2013)
48. H. Yu, B. Ratra, F.-Y. Wang, ApJ **856**(1), 3 (2018). arXiv:1711.03437
49. O. Farooq, F.R. Madiyar, S. Crandall, B. Ratra, ApJ **835**(1), 26 (2017). arXiv:1607.03537
50. A. Friedmann, Zeitsch. Phys. **21**, 326–332 (1924)
51. G. Lematre, Ann. Soc. Sci. Brux. **47**, 49–59 (1927)
52. H.P. Robertson, PNAS **15**(11), 822–829 (1929)
53. A.G. Walker, Proc. Lond. Math. Soc. **42**(2), 90–127 (1937)
54. S. Weinberg, *Gravitation and Cosmology: Principle and Applications of General Theory of Relativity* (Wiley, New York, 1972)
55. A.M. Velasquez-Toribio, M.L. Bedran, Braz. J. Phys. **41**, 59 (2011)
56. S. Nesseris, A. Shafieloo, MNRAS **408**, 1879 (2010). arXiv:1004.0960
57. M. Seikel, C. Clarkson, M. Smith, JCAP **06**, 036 (2012)
58. A.M. Velasquez-Toribio, M.M. Machado, J.C. Fabris, Eur. Phys. J. C **79**, 1010 (2019)
59. D.M. Scolnic et al., ApJ **859**(2), 101 (2018)
60. R. Tripp, A&A **331**, 815 (1998)
61. A. Conley, J. Guy, M. Sullivan et al., ApJ Supp. **192**, 1 (2011)
62. R. Arjona, W. Cardona, S. Nesseris, Phys. Rev. D **99**, 043516 (2019). arXiv:1811.02469
63. R. Jimenez, A. Loeb, ApJ **573**, 37 (2002)
64. X. Zheng, X. Ding, M. Biesiada, S. Cao, Z. Zhu, ApJ **825**, 17 (2016). arXiv:1604.07910
65. Lima, J.A.S., Jesus, J.F., Santos, R.C., Gill, M.S.S. arXiv:1205.4688
66. J.R. Gott III, M.S. Vogeley, S. Podariu, B. Ratra, ApJ **549**, 1 (2001). arXiv:astro-ph/0006103
67. G. Chen, B. Ratra, PASP **123**, 1127 (2011). arXiv:astro-ph/1105.5206
68. Y. Chen, S. Kumar, B. Ratra, ApJ **835**, 86 (2017). arXiv:1606.07316
69. Y. Wang, L. Xu, G.-B. Zhao, ApJ **849**, 84 (2017). arXiv:1706.09149
70. W. Lin, M. Ishak, Phys. Rev. D **96**, 083532 (2017). arXiv:1708.09813
71. T.M.C. Abbott et al., DES. MNRAS **480**, 3879 (2018). arXiv:1711.00403 [astro-ph.CO]
72. B.S. Haridasu, V.V. Lukovic, M. Moresco, N. Vittorio, JCAP **1810**, 015 (2018). arXiv: 1805.03595
73. X. Zhang, PASP **130**, 084502 (2018)
74. Zhang, X., and Huang, Q.G. arXiv:1812.01877
75. A. Dominguez et al., ApJ **885**, 137 (2019). arXiv:1903.12097
76. M. Rigault et al., ApJ **802**, 20 (2015). arXiv:1412.6501
77. B.R. Zhang et al., MNRAS **471**, 2254 (2017). arXiv:1706.07573
78. S. Dhawan, S.W. Jha, B. Leibundgut, A&A **609**, A72 (2017). arXiv:1707,00715
79. Arenas D. Fernandez et al., MNRAS **474**, 1250 (2018). arxiv:1710.05951
80. W.L. Freedman et al., ApJ **882**, 34 (2019). arXiv:1907.05922
81. W.L. Freedman et al., ApJ **891**, 57 (2020). arXiv:1908.00993
82. Zhang X., Huang Q.-G., preprint (2019). arXiv:1911.09439
83. K. Liao, A. Shafieloo, R. E. Keeley and E. V. Linder. arXiv:2002.10605
84. G. Alestas, L. Kazantzidis, L. Perivolaropoulos. arXiv:2004.08363